Whole-brain mapping of efferent projections of the anterior cingulate cortex in adult male mice

Wantong Shi[1], Man Xue[1], Fengyi Wu[2], Kexin Fan[3], Qi-Yu Chen[2,4], Fang Xu[2], Xu-Hui Li[1,4] [iD], Guo-Qiang Bi[2], Jing-Shan Lu[1,4] [iD], and Min Zhuo[1,4,5] [iD]

Abstract

The anterior cingulate cortex (ACC) is a key cortical region that plays an important role in pain perception and emotional functions. Previous studies of the ACC projections have been collected primarily from monkeys, rabbits and rats. Due to technological advances, such as gene manipulation, recent progress has been made in our understanding of the molecular and cellular mechanisms of the ACC-related chronic pain and emotion is mainly obtained from adult mice. Few anatomic studies have examined the whole-brain projections of the ACC in adult mice. In the present study, we examined the continuous axonal outputs of the ACC in the whole brain of adult male mice. We used the virus anterograde tracing technique and an ultrahigh-speed imaging method of Volumetric Imaging with Synchronized on-the-fly-scan and Readout (VISoR). We created a three-dimensional (3D) reconstruction of mouse brains. We found that the ACC projected ip-silaterally primarily to the caudate putamen (CPu), ventral thalamic nucleus, zona incerta (ZI), periaqueductal gray (PAG), superior colliculus (SC), interpolar spinal trigeminal nucleus (Sp5I), and dorsal medullary reticular nucleus (MdD). The ACC also projected to contralateral brain regions, including the ACC, reuniens thalamic nucleus (Re), PAG, Sp5I, and MdD. Our results provide a whole-brain mapping of efferent projections from the ACC in adult male mice, and these findings are critical for future studies of the molecular and synaptic mechanisms of the ACC and its related network in mouse models of brain diseases.

Keywords

Anterior cingulate cortex, Efferent projections, Whole-brain mapping, VISoR, 3D reconstruction, Mice

[1]Center for Neuron and Disease, Frontier Institutes of Science and Technology, Xi'an Jiaotong University, China
[2]CAS Key Laboratory of Brain Connectome and Manipulation, Interdisciplinary Center for Brain Information, The Brain Cognition and Brain Disease Institute; Shenzhen-Hong Kong Institute of Brain Science-Shenzhen Fundamental Research Institutions, Shenzhen Institute of Advanced Technology, Chinese Academy of Sciences Shenzhen Institute of Advanced Technology, China
[3]The Institute of Molecular and Translational Medicine, Department of Biochemistry and Molecular Biology, School of Basic Medical Sciences, Xi'an Jiaotong University Health Science Center, China
[4]Institute of Brain Research, Qingdao International Academician Park, China
[5]Department of Physiology, Faculty of Medicine, Medical Science Building, University of Toronto, Toronto, Ontario, Canada

Corresponding Authors:
Jing-Shan Lu, Center for Neuron and Disease, Frontier Institutes of Science and Technology, Xi'an Jiaotong University, Center for Neuron and Disease, Xi'an, Shaanxi 710049, China.
Email: lujs33@mail.xjtu.edu.cn

Min Zhuo, Institute of Brain Research, Qingdao International Academician Park, 1 King's College CircleQingdao, Toronto, Ontario, M5S 1A8, Canada.
Email: minzhuo10@gmail.com

Introduction

The anterior cingulate cortex (ACC) has been shown to play a critical role in pain perception and emotional responses.[1-4] The ACC exerts different functions through its projection to different cortical and subcortical areas.[5,6] Anatomical studies of the ACC projections have predominantly been collected from monkeys,[7,8] rabbits,[9-11] cats,[12] and rats.[13,14] For example, previous studies in monkeys have found that the ACC projected to the temporal cortex, striatum, thalamus, and basolateral amygdala (BLA).[7, 8] Recently, studies of the ACC molecular and synaptic mechanisms, such as long-term potentiation (LTP) and long-term depression (LTD), have been performed in adult mice.[1-3,6] Chen et al. reported that stimulation of the ACC directly enhanced spinal excitatory synaptic transmission through the direct ACC-spinal projection pathway.[15,16] Less is known about the ACC efferent in adult mice.

In the past, fluorescence imaging of serial thin brain slices was used to study brain connections.[17] This method requires proportional sampling due to the thin and large number of sections, which results in a lack of continuity and resolution of axonal tracing. Recently, Bi group developed an efficient whole-brain imaging method of Volumetric Imaging with Synchronized on-the-fly-scan and Readout (VISoR) for brain mapping. By semi-automated three-dimensional (3D) reconstruction, versatile high-throughput cell-type-specific 3D whole-brain mapping can be achieved quickly. This method has been used to study thalamocortical projection mapping of monkey brains and whole-brain imaging of neuronal activation in mice under the forced swimming conditions.[18,19] The VISoR technique overcame several key technical challenges to enable high resolution, high throughput and scalability whole-brain mapping, and provided a better view of long-range projections.

Recently, we used rabies virus-based retrograde virus and combined the VISoR method to map thalamic-ACC monosynaptic inputs in adult mice.[20] In the present study, we mapped the whole-brain outputs of the ACC in adult male mice by applying the anterograde virus into the unilateral ACC and following by VISoR imaging technique and 3D reconstruction. By tracing the ACC efferents, we found that the ACC mainly projected to ipsilateral nuclei, while a small number of fibers projected to some contralateral nuclei in adult male mice.

Materials and Methods

Animals

Adult (8–12 weeks old) male C57BL/6 mice were purchased from the Experimental Animal Center of Xi'an Jiaotong University. All animals were randomly housed under an artificial 12 h light/dark cycle (9 a.m.–9 p.m. light) with food and water provided *ad libitum*. All experimental protocols were approved by the Ethics Committee of Xi'an Jiaotong University.

Virus anterograde tracing

To analyze the efferent projections from the ACC in mice, we micro-injected 200 nL of the rAAV-hSyn-EGFP-2a-WPREs-pA (AAV2/9, 2.0×10^{12} genomics copies per mL; Brainvta company, Wuhan, China) into the unilateral ACC. Briefly, four mice were anesthetized with 2% isoflurane and placed in a stereotaxic device. The virus was injected by a glass pipette and microsyringe pump (23 nL/min, once every 10 s; Nanoject II #3-000-205/206, DRUMMOND) into the right ACC according to the 4th edition of the mouse brain atlas (0.9 mm anterior to bregma, 0.3 mm lateral to the midline, 1.4 mm deep from the cerebral surface). After injection, the surgical wound was carefully sutured and disinfected. The animals were monitored until waking up before returning to their home cages. Mice were allowed to survive for approximately 3–4 weeks for virus expression.[16,21]

Perfusion and slice preparation

Four weeks after viral expression, mice were deeply anesthetized with 2% isoflurane and perfused intracardially with 0.01 M phosphate-buffered saline (PBS, pH 7.4) followed by 4% w/v paraformaldehyde (PFA, pH 7.4). The brain was removed and incubated in 4% hydrogel monomer solution (HMS, 4% w/v acrylamide, 0.05% w/v bisacrylamide, 1× PBS, 4% w/v PFA, 0.25% VA-044 thermal initiator, and distilled water) at 4°C for 2 days, to allow penetration of fixation solution.

The sample was embedded with an equal volume mixture of 4% HMS and 20% bovine serum albumin (BSA) at 37°C for 4 h, and washed three times with PBS. The embedded block was trimmed to ensure that the sample was vertically glued to the base of the vibroslicer (Compresstome VF-300, Precisionary Instruments). Then, the brain was cut into 300-μm-thick coronal slices.

Sample clearing

Brain slices were then treated following the two-step PuClear clearing method to obtain uniform optical transparency through the 300-μm thickness.[18] Firstly, brain slices were placed in 5% PBS-Triton at 37°C and gently shaken for 24 h to increase membrane permeability. Next, these brain slices were placed on quartz slides and incubated in PuClear solution (50% iohexol, 23% urea, 11% 2,2′,2″-nitrilotriethanol, and 16% distilled water) with a refractive index of 1.52 for 4 h.

Fluorescence imaging and whole-brain image reconstruction

Cleared brain slices were imaged at $1 \times 1 \times 2.5 \ \mu m^3$ voxel resolution using the VISoR2 technique as described previously.[18] Synchronized beam-scan illumination and camera-frame readout generated a stack of image frames of the 45° oblique optical sections of the sample with the sample stage moving linearly in the *X*-direction.

Image volumes of each mouse brain slice were stitched with the custom software to automatedly reconstruct the
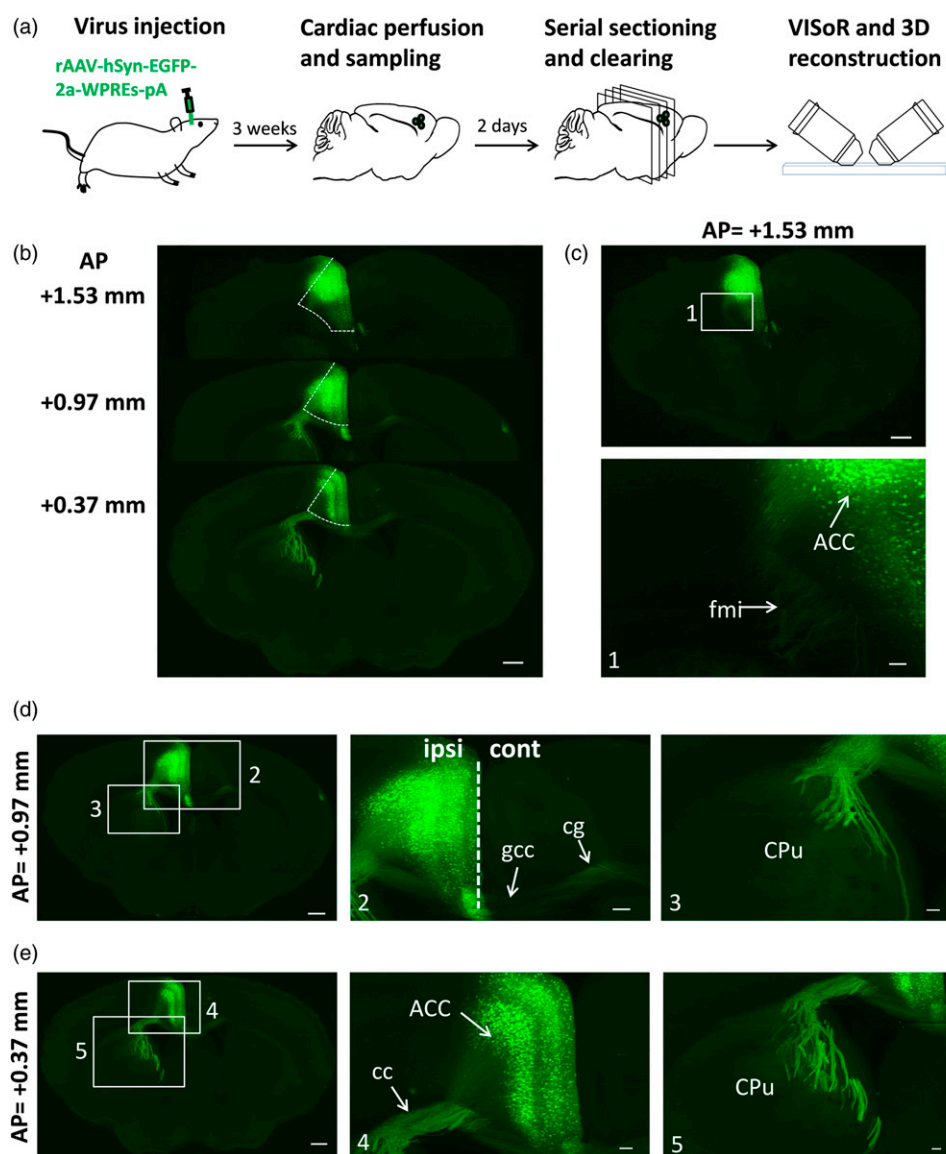
Figure 1. Expression of virus at the injection site and distribution of anterograde labeled fibers from the ACC in the CPu. (a) The procedure for anterograde tracing projections from the ACC. The rAAV-hSyn-EGFP-2a-WPREs-pA was injected unilaterally into the ACC of the mice. Three weeks after the injection of the virus, the whole mouse brain was sampled and sectioned for VISoR and 3D reconstruction. (b) Fluorescence images of the brain slices containing ACC after virus-injection into the ACC. (c) Virus-infected fibers were distributed in the fmi of the slice including the rostral ACC. The white box was augmented in 1. (d) Virus-infected fibers were distributed in the bilateral cc, gcc, and ipsilateral CPu. White boxes were augmented in 2 and 3. (e) Virus-infected fibers were distributed in the cc and CPu of the slice containing the caudal ACC. White boxes were augmented in 4 and 5. ACC, anterior cingulate cortex; fmi, forceps minor of the corpus callosum; ipsi, ipsilateral; cont, contralateral; gcc, genu of the corpus callosum; cg, cingulum; CPu, caudate putamen (striatum); cc, corpus callosum. Scale bars: b, top of c, left of d and e, 500 μm; 1, 80 μm; 2, 150 μm; 3–5, 100 μm.

whole brain as described previously.[18] The image volumes of the whole brain were then converted to the Imaris file format (IMS) for visualization and video rendering in Imaris software (v9.5, Oxford Instruments).

Results

To examine the whole-brain efferents of the ACC, we injected the anterograde virus into the right ACC of four adult male mice. This procedure is illustrated in Figure 1(a). The virus was expressed in the rostral to caudal ACC neurons (Figure 1(b)). These results suggested that the following brain regions with projection fibers were the targets of the ACC outputs. Following the areal nomenclature for cingulate regions was from the fourth edition of the mouse brain atlas. The general correspondence of nomenclature with the brain areas was as follows: area 25 corresponds to the infralimbic cortex (IL), area 32 to the prelimbic cortex (PrL), and area
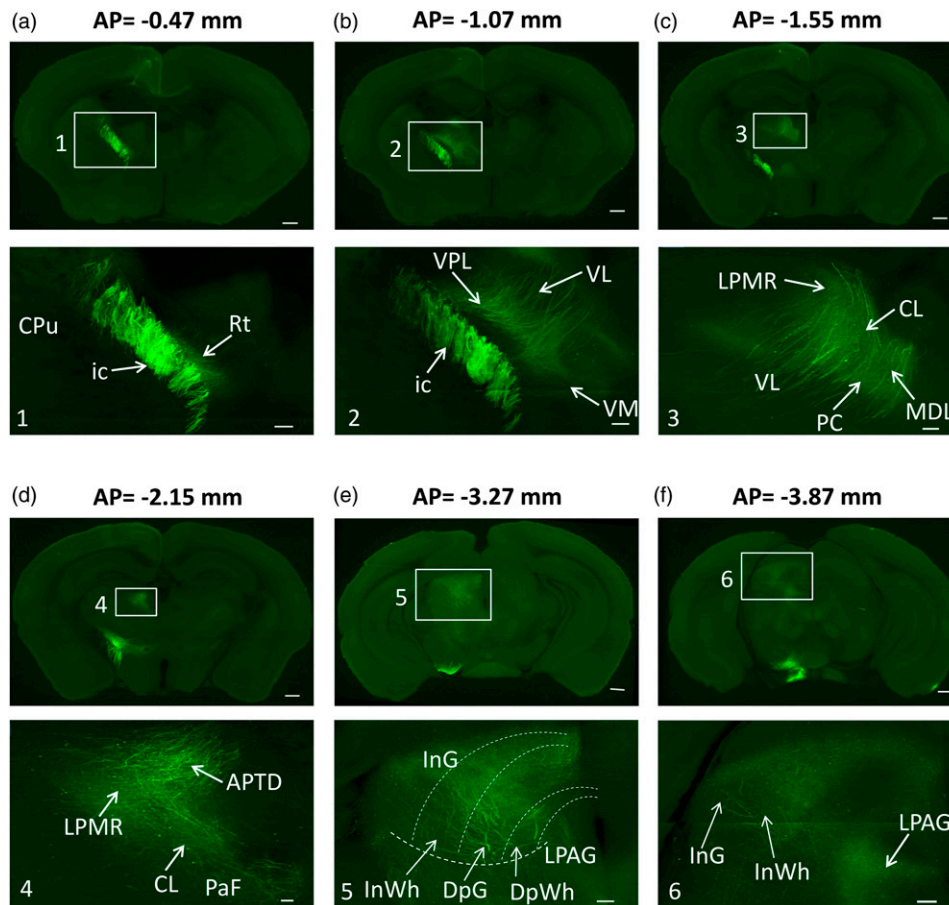
Figure 2. Distribution of anterograde labeled fibers from the ACC in the thalamus and SC. (a) Virus-infected fibers were distributed in the ic and Rt. The white box was augmented in 1. (b) Virus-infected fibers were distributed in the ic and the ventral thalamic nucleus. The white box was augmented in 2. (c) Virus-infected fibers were distributed in the VL, PC, MDL, CL, and LPMR of the thalamus. The white box was augmented in 3. (d) Virus-infected fibers were distributed in the CL, PaF and LPMR of the thalamus, and APTD of the pretectal nucleus. The white box was augmented in 4. (e) Virus-infected fibers were distributed in the InG, InWh, DpG and DpWh of the SC, and LPAG. The white box was augmented in 5. (f) Virus-infected fibers were distributed in the InG and InWh of the SC. The white box was augmented in 6. CPu, caudate putamen (striatum); ic, internal capsule; Rt, reticular nucleus; VM, ventromedial thalamic nucleus; VL, ventrolateral thalamic nucleus; VPL, ventral posterolateral thalamic nucleus; PC, paracentral thalamic nucleus; MDL, mediodorsal thalamic nucleus, lateral part; CL, centrolateral thalamic nucleus; LPMR, lateral posterior thalamic nucleus, mediorostral part; APTD, anterior pretectal nucleus, dorsal part; PaF, parafascicular thalamic nucleus; InG, intermediate gray layer of the superior colliculus; InWh, intermediate white layer of the superior colliculus; DpG, deep gray layer of the superior colliculus; DpWh, deep white layer of the superior colliculus; SC, superior colliculus; LPAG, lateral periaqueductal gray. Scale bars: top of a-f, 500 μm; 1, 2, 5, 6, 150 μm; 3, 100 μm; 4, 50 μm.

24a/24b to the ACC. The retrosplenial cortex (RSC) includes the retrosplenial agranular (RSA) and the retrosplenial granular cortex (RSG), corresponding to areas 30 and 29, respectively.

Distribution of projection fibers in the caudate putamen (CPu) and contralateral ACC from the ACC

The CPu is a key brain region that receives projections from the cortex.[22] The ACC to CPu inputs mediates histaminergic itch sensation.[23] Here, we observed the direct projection from the ACC to the CPu by whole-brain mapping of the ACC efferents in the adult mice. In the brain slice containing the rostral ACC, we found mildly labeled ACC projection fibers at the forceps minor of the corpus callosum (fmi) and its junction with the ACC (Figure 1(c)). In the middle ACC slice, the ipsilateral cingulum (cg), genu of the corpus callosum (gcc) and CPu displayed moderate labeling after the injection of anterograde virus into the ACC. In addition, mild labeling was observed in the contralateral cg and gcc, and very sparse labeling was also shown in the contralateral ACC (Figure 1(d)), indicating that the ACC sent direct projections to the contralateral ACC. In the slice containing the caudal ACC, the neurons of superficial and deep layers in the ACC were obviously infected by the anterograde virus. We also observed strong labeling in the ipsilateral corpus callosum (cc)
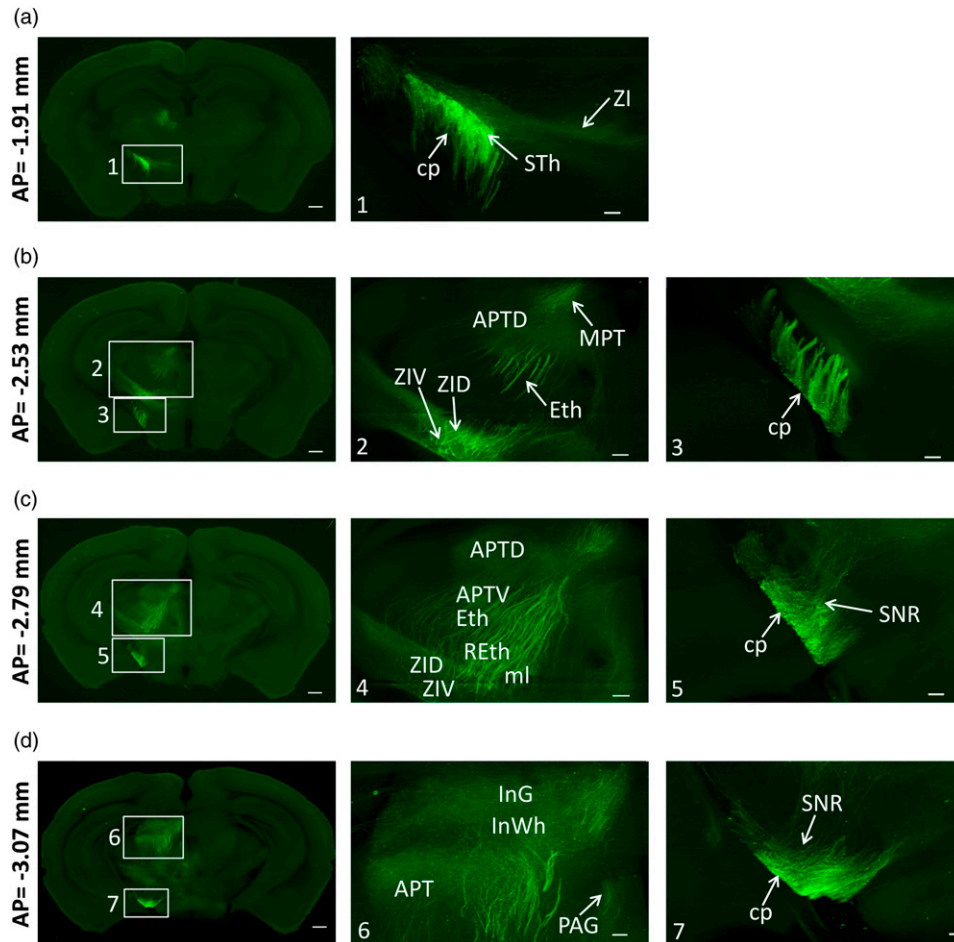
Figure 3. Distribution of anterograde labeled fibers from the ACC in the ZI, SC and cp. (a) Virus-infected fibers were distributed in the cp, STh and ZI. The white box was augmented in 1. (b) Virus-infected fibers were distributed in the ZI, pretectal area, and cp. White boxes were augmented in 2 and 3. (c) Virus-infected fibers were distributed in the ZI, thalamus, pretectal area and cp. White boxes were augmented in 4 and 5. (d) Virus-infected fibers were distributed in the pretectal area, SC, PAG and cp. White boxes were augmented in 6 and 7. cp, cerebral peduncle; STh, subthalamic nucleus; ZI, zona incerta; ZIV, zona incerta, ventral part; ZID, zona incerta, dorsal part; APTD, anterior pretectal nucleus, dorsal part; MPT, medial pretectal area; Eth, ethmoid thalamic nucleus; APTV, anterior pretectal nucleus, ventral part; REth, retroethmoid nucleus; ml, medial lemniscus; SNR, substantia nigra, reticular part; APT, anterior pretectal nucleus; PAG, periaqueductal gray; SC, superior colliculus; InG, intermediate gray layer of the superior colliculus; InWh, intermediate white layer of the superior colliculus. Scale bars: left of a-d, 500 μm; 1, 3, 5, 7, 100 μm; 2, 4, 6, 150 μm.

(Figure 1(e)). Compared with the middle ACC slice, the labeled fibers of the CPu were denser and more ventral in the caudal ACC slice (Figures 1(d) and (e)). These results indicate that the ACC projects to the ipsilateral cc and CPu, with a small number of projections to the contralateral ACC and cc.

Distribution of projection fibers in the thalamus and superior colliculus (SC) from the ACC

The thalamus and SC are two main targets of the ACC outputs.[8,21,24] In the brain slice containing the rostral thalamus, light labeling was found in the bilateral cc. The internal capsule (ic) received dense inputs from the ACC. The ACC projection fibers were lightly labeled in the reticular thalamic nucleus (Rt) (Figure 2(a)). In the brain slice containing the ventral thalamic nucleus, the projection fibers from the ACC divided into two major branches at the ic: the ventral branch ran along and across the ic, and the dorsal bundle of fibers distributed in the ventral thalamic nuclei, including the ventral posterolateral (VPL), ventrolateral (VL), and ventromedial (VM) thalamic nuclei (Figure 2(b)). In the more caudal brain slice, moderately labeled projection fibers were found in the VL, mediorostral part of the lateral posterior (LPMR), paracentral (PC), lateral part of mediodorsal (MDL), and centrolateral (CL) thalamic nucleus from the dorsal branch of the ic (Figure 2(c)). In the brain slice containing the caudal thalamus, in addition to light-labeled
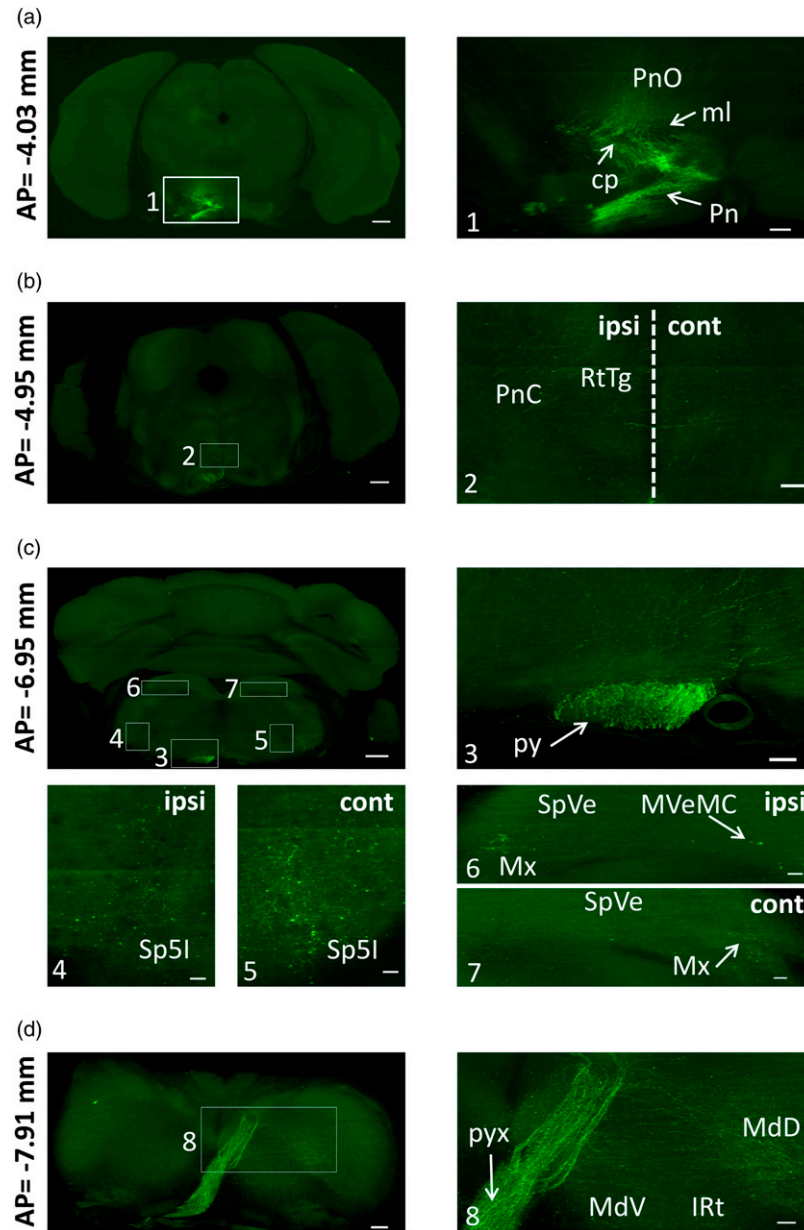
Figure 4. Distribution of anterograde labeled fibers from the ACC in the brainstem. (a) Virus-infected fibers were distributed in the cp, Pn, ml and PnO. The white box was augmented in 1. (b) Virus-infected fibers were bilaterally distributed in the PnC and RtTg. The white box was augmented in 2. (c) Virus-infected fibers were distributed in the ipsilateral py, SP5I, Mx, MVeMC, and contralateral SP5I, Mx, and SpVe. The white boxes were augmented in 3-7. (d) Virus-infected fibers were distributed in the pyx and MdD of contralateral. The white box was augmented in 8. cp, cerebral peduncle; Pn, pontine nuclei; ml, medial lemniscus; PnO, oral part of the pontine reticular nucleus; PnC, caudal part of the pontine reticular nucleus; RtTg, reticulotegmental nucleus of the pons; ipsi, ipsilateral; cont, contralateral; py, pyramidal tract; Sp5I, interpolar part of the spinal trigeminal nucleus; Mx, matrix region of the medulla; MVeMC, magnocellular of the medial vestibular nucleus; SpVe, spinal vestibular nucleus; pyx, pyramidal decussation; MdD, dorsal part of the medullary reticular nucleus; MdV, ventral part of the medullary reticular nucleus; IRt, intermediate reticular nucleus. Scale bars: left of a-d, 500 μm; 1, 150 μm; 2, 3, 100 μm; 4–7, 50 μm; 8, 80 μm.

fibers in the LPMR and CL of the thalamus, moderate labeling was also observed in the dorsal part of the anterior pretectal nuclei (APTD) (Figure 2(d)). Finally, the dorsal branch terminals were found in the SC, including the intermediate gray layer (InG), intermediate white layer (InWh), deep gray layer (DpG), and deep white layer (DpWh) of SC.

The periaqueductal gray (PAG) also received mild ACC projections (Figures 2(e) and 2(f)). Furthermore, the ACC projection fibers were also found in the ipsilateral anterior and posterior thalamic nuclear groups. We also found a small number of the ACC efferent fibers in the contralateral reuniens thalamic nucleus (Re) and PAG. Taken together, these

results suggest that the ACC projection fibers produce two major branches at ic, the dorsal branch passing through the ventral, medial, and central thalamus, and terminating to SC and PAG.

Distribution of projection fibers in the zona incerta (ZI) and cerebral peduncle (cp) from the ACC

ZI connects with many brain areas, which involves the modulation of behaviors and physiological states.[25] The cp consists of descending fibers from the cerebral cortex to the cerebellum, medulla oblongata, and spinal cord.[7] In the brain slice containing the caudal thalamus, we found that the ZI and cp received dense labeled fibers from the ACC, belonging to the ventral branch of the ic. The subthalamic nucleus (STh) between the ZI and cp was also labeled with dense fibers (Figure 3(a)). In the more caudal slice compared with Figure 3(a), the labeled ACC projection fibers were divided into two branches and projected to ZI and cp, respectively. In the ZI branch, the ventral (ZIV) and dorsal parts (ZID) of the ZI displayed strongly labeled fibers. In addition, APTD and medial pretectal nuclei (MPT) also received moderate inputs. The other branch had dense labeling at the cp (Figure 3(b)). In the more caudal slice compared with Figure 3(b), light-labeled fibers were found in the ZI, APTD, and ventral part of anterior pretectal nuclei (APTV). The medial lemniscus (ml), retroethmoid nucleus (REth), and ethmoid thalamic nucleus (Eth) showed dense labeling (Figure 3(c)). In the more caudal slice, InG and InWh of SC received moderate inputs, and the anterior pretectal nuclei (APT) and PAG received light inputs from the ACC (Figure 3(d)). In the cp branch of Figures 3(c) and (d), the cp and substantia nigra (SNR) displayed dense labeled fibers (Figures 3(c) and (d)). Furthermore, in the ZI branch, the ACC projection fibers were also found in the parafascicular thalamic nucleus (PaF) and posterior thalamic nuclear group. These results show that the ventral branch projection fibers at ic project to ZI and cp, respectively. In the ZI branch, ACC efferent fibers project to the posterior thalamus and APTD, and terminate in the SC and PAG. In the cp branch, ACC fibers project to the cp and SNR, and continue into the brainstem.

Distribution of projection fibers in the brainstem from the ACC

According to previous studies, the ACC had outputs to the midbrain, pons and medulla oblongata of the brainstem.[14,22] In Figure 3, the cp received strong ACC projections and continued to transmit the ACC outputs to other areas of the brainstem. In Figure 4(a), the cp, pontine nuclei (Pn), ml, and oral part of the pontine reticular nucleus (PnO) showed moderately labeled fibers from the ACC (Figure 4(a)). The brain slice containing the brainstem showed that the bilateral

caudal part of the pontine reticular nucleus (PnC) and reticulotegmental nucleus of the pons (RtTg) received sporadic inputs from the ACC (Figure 4(b)). In the more caudal slice compared with Figure 4(b), the ipsilateral pyramidal tract (py) displayed moderately labeled projection fibers from the ACC. Sporadic ACC projection fibers were transmitted to the bilateral interpolar spinal trigeminal nucleus (Sp5I), matrix region of the medulla (Mx), and spinal vestibular nucleus (SpVe) (Figure 4(c)). In the caudal brainstem, a dense bundle of the ACC fibers was observed in the contralateral pyramidal decussation (pyx), bilateral dorsal (MdD) and ventral (MdV) parts of the medullary reticular nucleus (Figure 4(d)). Furthermore, the ACC projection fibers were also found in the ventral pontine reticular nucleus (PnV), raphe magnus nucleus (RMg), gigantocellular reticular nucleus (Gi), paramedian reticular nucleus (PMn), and tegmental areas of midbrain and pons, and all of these projections were bilateral. The results suggest that the ACC projects to the brainstem through the cp and py, and the main targets are bilateral pons and reticular structures. ACC projection fibers are observed in the contralateral pyx, and it is likely that the ACC projects to the contralateral spinal cord through the pyx.

Distribution of projection fibers in the other cortical areas from the ACC

The ACC has direct connections with many other cerebral cortices, such as the motor cortex and visual cortex.[26,27] In the present study, many cortical areas had labeled efferent fibers from the ACC. The orbitofrontal cortex (OFC) is divided into three parts, including the medial (MO), ventral (VO), and lateral (LO) orbital cortices. Sparse labeling was observed in the OFC after injecting the anterograde virus into the ACC. The frontal association cortex (FrA) and PrL also displayed sparsely labeled projection fibers (Figure 5(a)). In the coronal slice shown in Figure 2(b), the RSA, RSG, primary somatosensory cortex (S1), primary (M1) and secondary (M2) motor cortex received light inputs from the ACC (Figures 5(b) and (c)). In addition, light labeling was found in the primary (V1) and secondary (V2) visual cortices (Figures 2(d) and 5(d)). These results show that the ACC projection fibers are found in many cortical areas, including orbitofrontal, prefrontal, retrosplenial, motor, somatosensory, and visual cortices, but the projection fibers are sparse and ipsilateral.

Discussion

The results of our present study show the whole-brain efferent projections of the ACC in the adult male mice by applying anterograde virus into the unilateral ACC. Through fluorescence imaging and 3D reconstruction, we found that a bundle of dense ACC projecting axons produces three major branches through the CPu and ic. The two branches project to the SC and PAG through the ventral thalamus and posterior
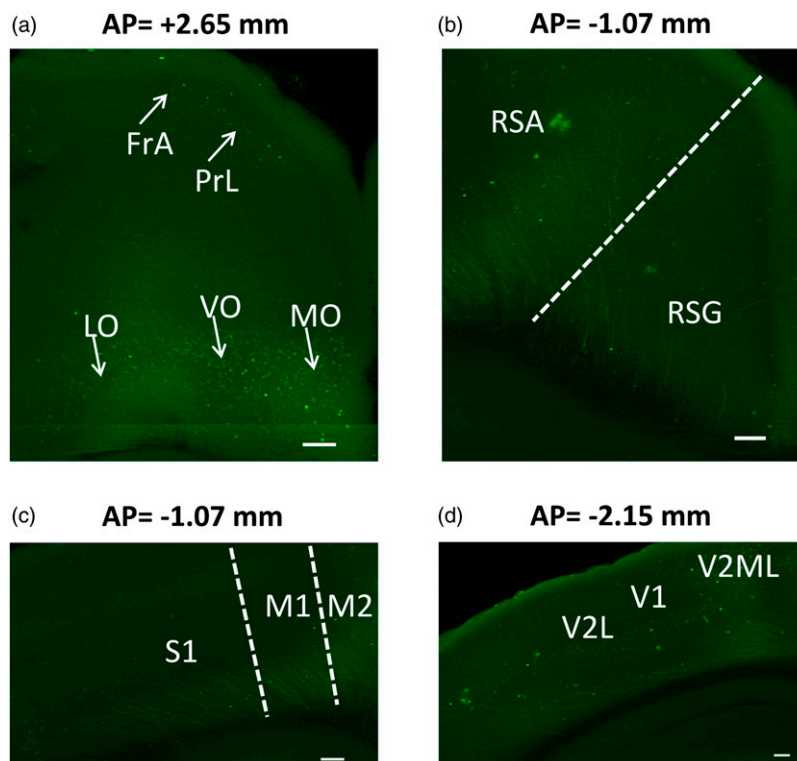
Figure 5. Distribution of anterograde labeled fibers from the ACC in the other cortical areas. (a-d) Light virus-infected fibers were distributed in the OFC, PrL, FrA (a), retrosplenial cortex (b), S1, M (c), and V (d) after the virus injection into the ACC. OFC, orbitofrontal cortex; LO, lateral orbital cortex; VO, ventral orbital cortex; MO, medial orbital cortex; PrL, prelimbic cortex; FrA, frontal association cortex; RSA, retrosplenial agranular cortex; RSG, retrosplenial granular cortex; S1, primary somatosensory cortex; M1, primary motor cortex; M2, secondary motor cortex; V1, primary visual cortex; V2L, lateral area of the secondary visual cortex; V2ML, mediolateral area of the secondary visual cortex. Scale bars: a, c, 150 μm; b, d, 100 μm.

thalamus, respectively. The other branch through the cp and py targets to the bilateral pons and medulla oblongata. In addition to subcortical projections, the ACC slightly projects to the cortical areas, such as the ispilateral orbitofrontal, prefrontal (PFC), motor, somatosensory, visual cortices, and the contralateral ACC (Figure 6).

Ipsilateral and contralateral projection from ACC

In our present study, most of the ACC fibers projected to the ipsilateral brain regions of the virus injection site, and a small amount to the contralateral ACC, Re, PAG, Sp5I, and MdD. Major targets of the ACC ipsilateral projection in mice included the CPu, ventral thalamic nuclei, ZI, PAG, SC, Sp5I, and MdD. Among them, the ACC projection to bilateral MdD is consistent with a previous study of rats.[28] In addition to MdD, ACC projections to other ipsilateral or contralateral brain regions have been reported in previous studies in mice[17,21,22] (Table 1). These anatomical connections may provide new perspectives for further study of the functions and mechanisms of ACC efferent pathways. For example, our results show that the ACC projects to the contralateral ACC. Hu et al.[29] revealed a circuit mechanism in which the cross-callosal projection of ACC-contralateral ACC contributes to mirror-image pain. However, other functions and

molecular mechanisms of the ACC-contralateral ACC pathway are not clear, so it is worth more research in the future.

ACC projection to the BLA and hippocampus

The BLA is an important brain region for emotional fear and anxiety. The ACC projection to the BLA has been found in monkeys, rabbits, and rats.[10,26,30] Previous studies have reported that the ACC inputs to the BLA control the fear response in mice.[31,32] Tang et al.[33] also demonstrated that direct stimulation of the ACC in mice produces fear behavior, and induces long-term auditory fear memory, which requires the activation of N-methyl-D-aspartate (NMDA) receptors in the BLA. The hippocampus is an important brain region associated with memory. A direct projection from the ACC to the hippocampus has also been found in rats and mice.[34,35] The ACC projection to the ventral hippocampus mediates contextual fear generalization.[35,36] Optogenetic manipulation of the ACC to hippocampus elicits contextual memory retrieval.[35] However, we did not observe any ACC projection to the BLA or hippocampus in the present study. We adjusted the fluorescent brightness and contrast, and found that the BLA and hippocampus still had no signal. Upon analysis, these inconsistent results may be
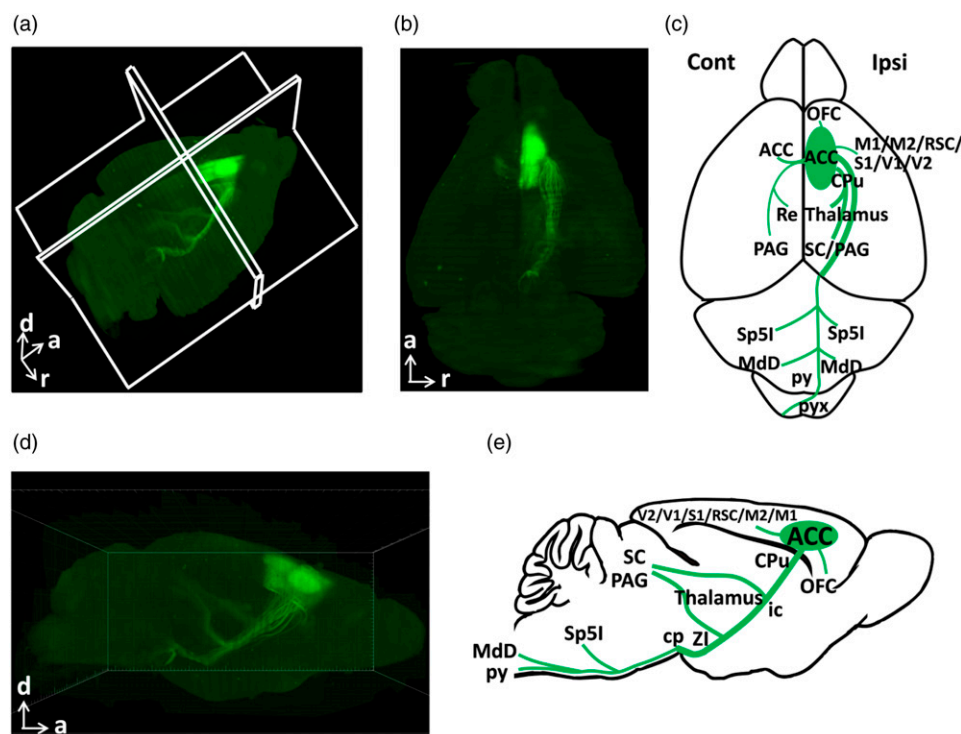
Figure 6. The 3D map and summary of anterograde labeled fibers from the ACC in the whole brain. (a, b, and d) The 3D (a), vertical (b), lateral (d) views of whole-brain distributions from ACC axons projected by VISoR and 3D reconstruction. (c and e) Shown are major brain areas and pathways in the ACC project network. ipsi, ipsilateral; cont, contralateral. d, dorsal; a, anterior; r, right; ACC, anterior cingulate cortex; OFC, orbitofrontal cortex; M1, primary motor cortex; M2, secondary motor cortex; RSC, retrosplenial cortex; S1, primary somatosensory cortex; V1, primary visual cortex; V2, secondary visual cortex; CPu, caudate putamen (striatum); Re, reuniens thalamic nucleus; PAG, periaqueductal gray; SC, superior colliculus; Sp5I, interpolar part of the spinal trigeminal nucleus; MdD, dorsal part of the medullary reticular nucleus; py, pyramidal tract; pyx, pyramidal decussation; ic, internal capsule; cp, cerebral peduncle; ZI, zona incerta.

Table 1. Summary of studies on bilateral efferents of the ACC.

Brain regions	Monkeys[7,8] Ispi	Cont	Rabbits[9-11] Ispi	Cont	Rats[13,14,28] Ispi	Cont	Mice[17,21,22] (previous studies) Ispi	Cont	Mice (present study) Ispi	Cont
ACC	+	−	+	−	+	−	+	+	+	+
M1/M2/CPu	+	−	+	−	+	−	+	+	+	−
BLA	+	−	+	−	+	−	+	+	−	−
LS/MS/VDB	−	−	−	−	−	−	+	+	−	−
Cl	−	−	+	+	−	−	+	+	−	−
Re/AM/IAD	+	−	+	+	+	+	+	+	+	+
PAG/VTA/MnR	+	−	+	+	+	−	+	+	+	+
LC/Pn/LDTg/CG	+	−	+	+	+	+	+	+	+	+
MdD/MdV	−	−	−	−	+	+	−	−	+	+

+: ACC efferent projections have been reported; −: ACC efferent projections have not been reported; Ipsi: ipsilateral; Cont: contralateral; ACC, anterior cingulate cortex; M1, primary motor cortex; M2, secondary motor cortex; CPu, caudate putamen (striatum); BLA, basolateral amygdaloid nucleus; LS, lateral septal nucleus; MS, medial septal nucleus; VDB, nucleus of the vertical limb of the diagonal band; Cl, claustrum; Re, reuniens thalamic nucleus; AM, anteromedial thalamic nucleus; IAD, interanterodorsal thalamic nucleus; PAG, periaqueductal gray; VTA, ventral tegmental area; MnR, median raphe nucleus; LC, locus coeruleus; Pn, pontine nuclei; LDTg, laterodorsal tegmental nucleus; CG, central gray; MdD, dorsal part of the medullary reticular nucleus; MdV, ventral part of the medullary reticular nucleus.

due to the insufficient infectiousness and expression time of the anterograde virus. Differences in the injection site and volume of the virus or tracer may also contribute to the inconsistent results. The specific reason is still unclear and requires more experiments to be explored and confirmed in the future.

ACC projection to the brainstem and spinal cord

The brainstem is one of the main target areas of the mouse ACC projections. In the brainstem, we found labeled fibers from the ACC in the SC, PAG, ventral tegmental area (VTA), and rostral ventromedial medulla (RVM). These results are consistent with many previous studies in rabbits, rats and mice.[10,14,22,37,38] The pathway of ACC to SC participates in avoidance behaviors and visual performance.[17,37] The PAG and RVM play important roles in the descending modulation of chronic pain.[2,39-41] The RVM is thought to be one of the key relays for descending modulation of spinal sensory transmission. Descending facilitation from the ACC, caused by electrical stimulation or chemical activation, apparently relayed at the RVM.[40] The projection from the ACC to the VTA contributes to neuropathic pain-evoked aversion, which has also been described in rats.[38] We show that the ACC neurons also form connections with the ventrolateral (Pr5VL) and dorsomedial parts (Pr5DM) of the principal sensory trigeminal nucleus, interpolar (Sp5I) and oral parts of the spinal trigeminal nucleus (Sp5O). It has been reported that the spinal trigeminal nucleus receives afferents from the orofacial nociceptor, which is important to the modulation of chronic neuropathic orofacial pain.[42] Our results showed that labeled fibers from the ACC in the MdD and MdV. MdD and MdV act as supraspinal pain regulatory areas to regulate the pain sensation process in the spinal cord.[43] Furthermore, a direct projection from the ACC to the spinal cord has been reported in rats and mice.[15,16,44] ACC output mapping was not performed in the spinal cord in our study. However, we found that the ACC projects to the contralateral pyx. It is likely that ACC projects to the contralateral spinal cord through pyx.

ACC projection to the other cortical areas

We observed that the ACC sends projections to many cortical areas, including ipsilateral orbitofrontal, prelimbic, retrosplenial, motor, somatosensory, and visual cortices (Figure 5). A previous study in monkeys showed that the pathway of the ACC to OFC affects perception and emotions.[45] The ACC projection to the PFC may influence sleep and cognition.[6,46] The ACC-M1 pathway regulates the motor activity of the orofacial and forelimb in rats.[47] A projection from the ACC to the visual cortex facilitates visual processing and improves visual discrimination.[37,48] In summary, the ACC connects with many other cortical areas, and these pathways regulate a variety of different functions.

Technical comparison

In the present study, we mapped the efferent projections from the ACC in mice using the VISoR system and 3D reconstruction. Previous reports have used 3D reconstructions to study brain structure and projection. For example, Zhang et al.[21] performed a 3D reconstruction of the brain region or pathway by continuously playing two-dimensional (2D) brain slices. However, this method does not produce a complete 3D image, which means it is impossible to observe the activity trace of the projection fibers. In addition, a previous study digitized projection fibers and then performed 3D reconstruction.[49] It is important to note that this method focuses on the anatomical distribution of the projection fibers, and thus, the intensity of the signal and details of the synaptic organization are not represented. We optimized tissue slicing and clearing, ultrahigh-speed imaging techniques, and efficient analysis tools.[19] The resulting 3D image clearly showed the details and pathway direction of axonal fibers. In summary, our results provide a more thorough understanding of the ACC efferent network in the mouse brain. This study creates an anatomical foundation for future studies on the pathways and functions of the ACC.

Authors' contributions

W.S. F.X., X.H.L., G.Q.B., J.S.L. and M.Z. designed the experiments. W.S., M.X., F.W. and K.F. preformed experiments and analyzed data. W.S., X.M., Q.Y.C, F.X., X.H.L., J.S.L. and M.Z. drafted the manuscript and finished the final version of the manuscript. All authors read and approved the final manuscript.

Code availability

Codes for VISoR2 image reconstruction are openly accessible at https://github.com/SMART-pipeline/Volume-reconstruction.

Data-availability statement

Original data is available from the corresponding authors upon reasonable request.

ORCID iDs

Xu-Hui Li https://orcid.org/0000-0003-4376-6252
Jing-Shan https://orcid.org/0000-0002-7330-6567
Min Zhuo https://orcid.org/0000-0001-9062-3241

References

1. Zhuo M. Cortical excitation and chronic pain. *Trends Neurosciences* 2008; 31: 199–207. DOI: 10.1016/j.tins.2008.01.003.

2. Zhuo M. Neural Mechanisms Underlying Anxiety-Chronic Pain Interactions. *Trends Neurosciences* 2016; 39: 136–145. DOI: 10.1016/j.tins.2016.01.006.

3. Zhuo M. Cortical plasticity as synaptic mechanism for chronic pain. *J Neural Transm* 2020; 127: 567–573. DOI: 10.1007/s00702-019-02071-3.

4. Vogt B. A. Submodalities of emotion in the context of cingulate subregions. *Cortex* 2014; 59: 197–202. DOI: 10.1016/j.cortex.2014.04.002.

5. Vogt B. A. Cingulate cortex in the three limbic subsystems. *Cingulate Cortex* 2019; 166: 39–51. DOI: 10.1016/B978-0-444-64196-0.00003-0.

6. Bliss T. V. P., Collingridge G. L., Kaang B.-K. and Zhuo M. Synaptic plasticity in the anterior cingulate cortex in acute and chronic pain. *Nat Rev Neurosci* 2016; 17: 485–496. DOI: 10.1038/nrn.2016.68.

7. Powell E. W. The cingulate bridge between allocortex, isocortex and thalamus. *Anatomical Rec* 1978; 190: 783–793.

8. Yeterian E. H. and Pandya D. N. Corticothalamic connections of paralimbic regions in the rhesus monkey. *J Comp Neurol* 1988; 269: 130–146.

9. Vogt B. A., Sikes R. W., Swadlow H. A. and Weyand T. G. Rabbit cingulate cortex: cytoarchitecture, physiological border with visual cortex, and afferent cortical connections of visual, motor, postsubicular, and intracingulate origin. *J Comp Neurol* 1986; 248: 74–94.

10. Buchanan S. L., Thompson R. H., Maxwell B. L. and Powell D. A. Efferent connections of the medial prefrontal cortex in the rabbit. *Exp Brain Res* 1994; 100: 469–483.

11. Weible A. P., Weiss C. and Disterhoft J. F. Connections of the caudal anterior cingulate cortex in rabbit: neural circuitry participating in the acquisition of trace eyeblink conditioning. *Neuroscience* 2007; 145: 288–302. DOI: 10.1016/j.neuroscience.2006.11.046.

12. Kaitz S. S. and Robertson R. T. Thalamic connections with limbic cortex. II. Corticothalamic projections. *J Comp Neurol* 1981; 195: 527–545.

13. Vogt B. A. and Miller M. W. Cortical connections between rat cingulate cortex and visual, motor, and postsubicular cortices. *J Comp Neurol* 1983; 216: 192–210.

14. Leichnetz G. R., Hardy S. G. P. and Carruth M. K. Frontal projections to the region of the oculomotor complex in the rat: a retrograde and anterograde HRP study. *J Comp Neurol* 1987; 263: 387–399.

15. Chen T, Taniguchi W., Chen Q.-Y., Tozaki-Saitoh H., Song Q., Liu R.-H., Koga K., Matsuda T., Kaito-Sugimura Y., Wang J., Li Z.-H., Lu Y.-C., Inoue K., Tsuda M., Li Y.-Q., Nakatsuka T. and Zhuo M. Top-down descending facilitation of spinal sensory excitatory transmission from the anterior cingulate cortex. *Nat Commun* 2018; 9: 1886. DOI: 10.1038/s41467-018-04309-2.

16. Chen T, Koga K, Descalzi G, Qiu S, Wang J, Zhang LS, Zhang ZJ, He XB, Qin X, Xu FQ, Hu J, Wei F, Huganir RL, Li YQ and Zhuo M. Postsynaptic potentiation of corticospinal projecting neurons in the anterior cingulate cortex after nerve injury. *Mol Pain* 2014; 10: 33.

17. Savage M. A., McQuade R. and Thiele A. Segregated fronto-cortical and midbrain connections in the mouse and their relation to approach and avoidance orienting behaviors. *J Comp Neurol* 2017; 525: 1980–1999. DOI: 10.1002/cne.24186.

18. Xu F., Shen Y., Ding L., Yang C.-Y., Tan H., Wang H., Zhu Q., Xu R., Wu F., Xiao Y., Xu C., Li Q., Su P., Zhang L. I., Dong H.-W., Desimone R., Xu F., Hu X., Lau P.-M. and Bi G.-Q. High-throughput mapping of a whole rhesus monkey brain at micrometer resolution. *Nat Biotechnol* 2021; 39: 1521–1528. DOI: 10.1038/s41587-021-00986-5.

19. Wang H., Zhu Q., Ding L., Shen Y., Yang C.-Y., Xu F., Shu C., Guo Y., Xiong Z., Shan Q., Jia F., Su P., Yang Q.-R., Li B., Cheng Y., He X., Chen X., Wu F., Zhou J.-N., Xu F., Han H., Lau P.-M. and Bi G.-Q. Scalable volumetric imaging for ultrahigh-speed brain mapping at synaptic resolution. *Natl Sci Rev* 2019; 6: 982–992. DOI: 10.1093/nsr/nwz053.

20. Xue M., Shi W., Zhou S., Li Y., Wu F., Chen Q.-Y., Liu R.-H., Zhou Z., Zhang Y.-X., Chen Y., Xu F., Bi G., Li X., Lu J. and Zhuo M. Mapping thalamic-anterior cingulate monosynaptic inputs in adult mice. *Mol Pain* 2022: 174480692210870. DOI: 10.1177/17448069221087034.

21. Zhang S., Xu M., Chang W.-C., Ma C., Hoang Do J. P., Jeong D., Lei T., Fan J. L. and Dan Y. Organization of long-range inputs and outputs of frontal cortex for top-down control. *Nat Neurosci* 2016; 19: 1733–1742. DOI: 10.1038/nn.4417.

22. Fillinger C., Yalcin I., Barrot M. and Veinante P. Efferents of anterior cingulate areas 24a and 24b and midcingulate areas 24a′ and 24b′ in the mouse. *Brain Struct Funct* 2018; 223: 1747–1778. DOI: 10.1007/s00429-017-1585-x.

23. Lu Y.-C., Wang Y.-J., Lu B., Chen M., Zheng P. and Liu J.-G. ACC to Dorsal Medial Striatum Inputs Modulate Histaminergic Itch Sensation. *J Neurosci* 2018; 38: 3823–3839. DOI: 10.1523/JNEUROSCI.3466-17.2018.

24. Vertes R. P. Analysis of projections from the medial prefrontal cortex to the thalamus in the rat, with emphasis on nucleus reuniens. *J Comp Neurol* 2002; 442: 163–187. DOI: 10.1002/cne.10083.

25. Wang X., Chou X.-l., Zhang L. I. and Tao H. W. Zona Incerta: An Integrative Node for Global Behavioral Modulation. *Trends Neurosciences* 2020; 43: 82–87. DOI: 10.1016/j.tins.2019.11.007.

26. Calderazzo S. M., Busch S. E., Moore T. L., Rosene D. L. and Medalla M. Distribution and overlap of entorhinal, premotor, and amygdalar connections in the monkey anterior cingulate cortex. *J Comp Neurol* 2021; 529: 885–904. DOI: 10.1002/cne.24986.

27. Zingg B., Hintiryan H., Gou L., Song M. Y., Bay M., Bienkowski M. S., Foster N. N., Yamashita S., Bowman I., Toga A. W. and Dong H.-W. Neural networks of the mouse

neocortex. *Cell* 2014; 156: 1096–1111. DOI: 10.1016/j.cell.2014.02.023.

28. Sesack S. R., Deutch A. Y., Roth R. H. and Bunney B. S. Topographical organization of the efferent projections of the medial prefrontal cortex in the rat: An anterograde tract-tracing study withPhaseolus vulgaris leucoagglutinin. *J Comp Neurol* 1989; 290: 213–242.

29. Hu S.-W., Zhang Q., Xia S.-H., Zhao W.-N., Li Q.-Z., Yang J.-X., An S., Ding H.-L., Zhang H. and Cao J.-L. Contralateral Projection of Anterior Cingulate Cortex Contributes to Mirror-Image Pain. *J Neurosci* 2021; 41: 9988–10003. DOI: 10.1523/JNEUROSCI.0881-21.2021.

30. Gabbott P. L. A., Warner T. A., Jays P. R. L., Salway P. and Busby S. J. Prefrontal cortex in the rat: projections to sub-cortical autonomic, motor, and limbic centers. *J Comp Neurol* 2005; 492: 145–177. DOI: 10.1002/cne.20738.

31. Jhang J., Lee H., Kang M. S., Lee H.-S., Park H. and Han J.-H. Anterior cingulate cortex and its input to the basolateral amygdala control innate fear response. *Nat Commun* 2018; 9: 2744. DOI: 10.1038/s41467-018-05090-y.

32. Smith M. L., Asada N. and Malenka R. C. Anterior cingulate inputs to nucleus accumbens control the social transfer of pain and analgesia. *Science* 2021; 371: 153–159. DOI: 10.1126/science.abe3040.

33. Tang J, Ko S, Ding HK, Qiu CS, Calejesan AA and Zhuo M. Pavlovian fear memory induced by activation in the anterior cingulate cortex. *Mol Pain* 2005; 1: 6. DOI: 10.1186/1744-8069-1-6.

34. Prasad J. A. and Chudasama Y. Viral tracing identifies parallel disynaptic pathways to the hippocampus. *J Neurosci* 2013; 33: 8494–8503. DOI: 10.1523/JNEUROSCI.5072-12.2013.

35. Rajasethupathy P., Sankaran S., Marshel J. H., Kim C. K., Ferenczi E., Lee S. Y., Berndt A., Ramakrishnan C., Jaffe A., Lo M., Liston C. and Deisseroth K. Projections from neocortex mediate top-down control of memory retrieval. *Nature* 2015; 526: 653–659. DOI: 10.1038/nature15389.

36. Bian X.-L., Qin C., Cai C.-Y., Zhou Y., Tao Y., Lin Y.-H., Wu H.-Y., Chang L., Luo C.-X. and Zhu D.-Y. Anterior Cingulate Cortex to Ventral Hippocampus Circuit Mediates Contextual Fear Generalization. *J Neurosci* 2019; 39: 5728–5739. DOI: 10.1523/JNEUROSCI.2739-18.2019.

37. Zhang S., Xu M., Kamigaki T., Hoang Do J. P., Chang W.-C., Jenvay S., Miyamichi K., Luo L. and Dan Y. Long-range and local circuits for top-down modulation of visual cortex processing. *Science* 2014; 345: 660–665.

38. Gao S.-H., Shen L.-L., Wen H.-Z., Zhao Y.-D., Chen P.-H. and Ruan H.-Z. The projections from the anterior cingulate cortex to the nucleus accumbens and ventral tegmental area contribute to neuropathic pain-evoked aversion in rats. *Neurobiol Dis* 2020; 140: 104862. DOI: 10.1016/j.nbd.2020.104862.

39. Zhuo M. Descending facilitation. *Mol Pain* 2017; 13: 1744806917699212. DOI: 10.1177/1744806917699212.

40. Calejesan A. A., Kim S. J. and Zhuo M. Descending facilitatory modulation of a behavioral nociceptive response by stimulation in the adult rat anterior cingulate cortex. *Eur J Pain* 2000; 4: 83–96. DOI: 10.1053/eujp.1999.0158.

41. Zhuo M. and Gebhart G. F. Facilitation and attenuation of a visceral nociceptive reflex from the rostroventral medulla in the rat. *Gastroenterology* 2002; 122: 1007–1019. DOI: 10.1053/gast.2002.32389.

42. Mills E. P., Di Pietro F., Alshelh Z., Peck C. C., Murray G. M., Vickers E. R. and Henderson L. A. Brainstem Pain-Control Circuitry Connectivity in Chronic Neuropathic Pain. *J Neurosci* 2018; 38: 465–473. DOI: 10.1523/JNEUROSCI.1647-17.2017.

43. Leite-Almeida H., Valle-Fernandes A. and Almeida A. Brain projections from the medullary dorsal reticular nucleus: an anterograde and retrograde tracing study in the rat. *Neuroscience* 2006; 140: 577–595. DOI: 10.1016/j.neuroscience.2006.02.022.

44. Miller MW. The origin of corticospinal projection neurons in rat. *Exp Brain Research* 1987; 67: 339–351.

45. García-Cabezas M. Á. and Barbas H. Anterior Cingulate Pathways May Affect Emotions Through Orbitofrontal Cortex. *Cereb Cortex* 2017; 27: 4891–4910. DOI: 10.1093/cercor/bhw284.

46. Medalla M. and Barbas H. The anterior cingulate cortex may enhance inhibition of lateral prefrontal cortex via m2 cholinergic receptors at dual synaptic sites. *J Neurosci* 2012; 32: 15611–15625. DOI: 10.1523/JNEUROSCI.2339-12.2012.

47. Wang Y., Matsuzaka Y., Mushiake H. and Shima K. Spatial distribution of cingulate cortical cells projecting to the primary motor cortex in the rat. *Neurosci Res* 2008; 60: 406–411. DOI: 10.1016/j.neures.2007.12.012.

48. Huda R., Sipe G. O., Breton-Provencher V., Cruz K. G., Pho G. N., Adam E., Gunter L. M. and Sullins A., Wickersham I. R. and Sur M. Distinct prefrontal top-down circuits differentially modulate sensorimotor behavior. *Nat Commun* 2020; 11: 6007. DOI: 10.1038/s41467-020-19772-z.

49. Atlan G., Terem A., Peretz-Rivlin N., Groysman M. and Citri A. Mapping synaptic cortico-claustral connectivity in the mouse. *J Comp Neurol* 2017; 525: 1381–1402. DOI: 10.1002/cne.23997.